# Effect of char on the combustion process of multicomponent bio-fuel

Amir Houshang Mahmoudi[a], A.K. Pozarlik[a], E. van der Weide[b], S.R.A. Kersten[c], S. Luding[d], G. Brem[e]

[a]*Thermal Engineering, University of Twente, The Netherlands*
[b]*Engineering Fluid Dynamics, University of Twente, The Netherlands*
[c]*Sustainable Process Technology, University of Twente, The Netherlands*
[d]*Multi Scale Mechanics, University of Twente, The Netherlands*
[e]*Energy Technology, University of Twente, The Netherlands*

**Abstract**

Combustion of pyrolysis oil has attracted many attention in recent years as a renewable and environmental friendly fuel. However, pyrolysis oil as an multi-component fuel has some differences compared to conventional fossil fuels. One of the main differences is the formation of solid char in the droplet during evaporation. The goal of this work is to study the effect of the solid char on the combustion characteristics of multi-component fuel. An Euler-Lagrange model of three phase gas/liquid/solid combustion is developed to study the detailed information about every phenomena in the process such as: heat, mass and momentum transfer between droplet and gas phase, droplet evaporation, homogeneous and heterogeneous reactions. The results indicate that the presence of the solid char and consequently its combustion elongates significantly the combustion region in a typical spray injection chamber/burner. Moreover, the gas phase reaches higher temperatures as a result of char combustion that creates more heat by heterogeneous oxidation as a kind of afterburner.

*Keywords:* Multiphysics numerical modeling, Euler-Lagrange models, Spray combustion, Multi-component fuel, Char formation

## 1. Introduction

The worldwide concern regarding global warming has increased the interest of using biomass as a renewable and $CO_2$ neutral source of energy. However, thermally liquefied biomass has a multicomponent nature and it is difficult to use in conventional combustion systems. Pyrolysis oil, as one of the most important products of biomass conversion, has the potential to be used as a fuel oil substitute in many applications for heat or electricity generation. A comprehensive literature review on the application of bio-oil has been done by S.Y. No [1]. However, pyrolysis-oil properties and its behavior during combustion are considerably different from conventional fossil fuels. From a chemical point of view, pyrolysis oil contains a large number of oxygenated compounds derived from the decomposition of biomass components during thermal treatment. It

*Email address:* a.mahmoudi@utwente.nl, amirhoshangm@gmail.com (Amir Houshang Mahmoudi)

has also considerable amount of water originating from both moisture content and decomposition reactions. Water is homogeneously dissolved in the oil and cannot be eliminated by drying processes without losing volatile hydrocarbon compounds [2]. From the physical properties point of view, bio-oils are characterized by high viscosity and surface tension, low heating value and, due to multicomponent composition, a very wide boiling range [3]. Moreover, they are thermally unstable and, when heated, undergo polymerization processes, leading to the formation of carbonaceous solid material (char) in the fuel's supply lines, at the injection nozzles' tip and in the combustion chambers [2]. Van Rossum et al. [4, 5] found that pyrolysis oil evaporation is always coupled to the formation of char. This represents one of the most severe obstacles for a direct use of pyrolysis oils in furnaces or diesel engines.

Different models have been proposed for the evaporation of bio-oil droplets [6, 7, 8, 9, 10, 11]. Hallett and Clark [6] presented a numerical model based on a continuous thermodynamics theory to calculate the evaporation of biomass pyrolysis oil droplets. They assumed a multicomponent mixture for the modeling of pyrolysis oil. In the model, one of the components (pyrolytic lignin) which has high molecular weight, in addition of evaporation was assumed to pyrolyze, producing char and gas. This was taken into account with a one-step first order reaction. Zhang et al. [8] proposed a numerical model with the continuous thermodynamics approach for vaporization of bio-oil, mixed with other practical fuels, including diesel fuel, biodiesel and ethanol. They found the lifetime of pure bio-oil drops is longer than diesel, biodiesel, and ethanol. Hence, the presence of bio-oil in the fuel mixture extends the drop lifetime. Yin [11] proposed a 2D axisymmetric model to study evaporation of bio-oil droplets. Yin used a finite volume method to numerically solve the flow, heat and mass transfer within the droplet and validated the model against analytical solutions and experimental data of ingle-component droplet evaporation.

There have been several experimental studies investigating the combustion behavior of pyrolysis oil [12, 13, 14, 15, 16, 17]. Wornat et al. [12] used single droplets (320 $\mu m$) from two biomass oils, produced from the pyrolysis of oak and pine. Different stages of the droplet's combustion life time were depicted by in-situ images and were explained in detail. Beran and Axelsson [16] studied experimentally pyrolysis oil combustion in a tubular combustor. Their results have been compared to the results obtained from ethanol and diesel combustion. They found that it is possible to burn pure pyrolysis oil in the load range between 70% and 100% with a combustion efficiency exceeding 99% and without the creation of sediments on the combustor inner wall. Hristov et al. [18] used an analytical model to study the bio-oil droplet combustion focusing on the heating period before droplet micro-explosion. Based on the analysis of the droplet combustion history, it was found that the diffusion limit model with a volumetric heating source and Stefan boundary condition is suitable to model the initial stages of droplet combustion. Sallevelt [19, 20] studied numerically the spray combustion of pyrolysis oil in a gas turbine. The effect of droplet size on the combustion characteristics was investigated in Ansys Fluent using an Eulerian-Lagrangian approach. Qualitatively good agreement with the experimental data was obtained. However, char formation and oxidation were neglected.

A literature survey indicates that combustion behavior of pyrolysis oil is still an unknown process. More investigations are required to understand pyrolysis oil spray formation, evaporation and combustion. Especially, the impact of char formation on the combustion characteristics, which has not been explored yet, needs detailed assessment. Knowledge and data about the specifics of the processes and phenomena which interact during the combustion of pyrolysis oil will support the design of a new generation of burners operating efficiently on this bio-fuel. The objective of this work is to investigate multicomponent oil combustion, including mutual interactions between gaseous, liquid and solid fields. A numerical model that takes into account

liquid fuel evaporation and gaseous and char combustion has been developed in OpenFOAM®. The char is considered to be present in the fuel droplets and its oxidation is modeled after the complete evaporation of the liquid.

## 2. Mathematical model

A numerical model for combustion of multicomponent and multiphase fuels has been implemented into the open source CFD package OpenFOAM® using the Eulerian-Lagrangian formulation. The gas phase is modeled as a continuous phase whereas each particle/droplet is tracked with a Lagrangian approach. A two way heat, mass and momentum exchange is applied between particles and gas phase which results in a strong coupling between the Eulerian and Lagrangian domains. Each particle/droplet consists of two phases (liquid and solid), while it interacts with the surrounding gas phase by heat, mass and momentum transfer.

Due to the small particle/droplet size and low Biot number, the intra-particle gradient of temperature and species is neglected [21]. The energy balance within a particle is given by

$$m\, C_{p_{eff}}\, \frac{dT_p}{dt} = h_\infty\, A_p\, (T_\infty - T_p) + \dot{q}_{eva} + \dot{q}_{comb} \tag{1}$$

where $\dot{q}_{eva}$, $\dot{q}_{comb}$, $T_p$, $T_\infty$ and $m$ are the energy consumption by evaporation, heat release by solid combustion, particle temperature, ambient gas temperature and particle mass, respectively. $A_p$ is the outer surface area of the particle and $C_{p_{eff}}$ is the effective heat capacity of the particle (considering both liquid and solid phases). The convective heat transfer coefficient ($h_\infty$) is calculated based on the Ranz-Marshall correction for the Nusselt number [22].

$$Nu = 2 + 0.6\, Re^{0.5} Pr^{0.33} \tag{2}$$

The Spalding evaporation model [23] is used to calculate the mass evolution of each liquid species in the particle.

$$\frac{dm_{p,i}}{dt} = -\pi\, d_p\, Sh\, \rho_{s,i}\, D_i\, ln(1 + B_M) \tag{3}$$

where $d_p$, $\rho_{s,i}$, $D_i$, $Sh$ and $m_{p,i}$ are the particle diameter, vapor density of species $i$ at the particle surface, diffusion coefficient of species $i$, Sherwood number and mass of species i, respectively. $B_M$ is the Spalding number, which is defined as:

$$B_M = \frac{Y_{s,i} - Y_{\infty,i}}{1 - Y_{s,i}} \tag{4}$$

where $Y_{s,i}$ and $Y_{\infty,i}$ are the mass fraction of species i at the particle surface and at ambient condition, respectively.

When the liquid phase in the particle evaporates completely, the solid residual might undergo a heterogeneous reaction.

$$Char + O_2 \rightarrow CO_2 \tag{5}$$

The reaction rate is calculated as follows [24]:

$$K_{kin} = A\, e^{\frac{-E}{RT}} \tag{6}$$

$$K_{diff} = B/d_p(\frac{T_p + T_\infty}{2})^{0.75} \tag{7}$$

$$\frac{dm_c}{dt} = A_p P_{O_2} \frac{1}{\frac{1}{K_{kin}} + \frac{1}{K_{diff}}} \tag{8}$$

where $P_{O_2}$, $K_{kin}$ and $K_{diff}$ are the partial pressure of oxygen and the kinetic and diffusion rates. The values of $A$, $E$ and $B$ are 0.002, $7.9 \times 10^7$ and $5 \times 10^{-12}$, respectively.

Van Rossum et al. [4] observed that some amount of solid char is always produced during the evaporation of pyrolysis oil (in range of 8% - 30%, carbon basis). The amount of char formation is proportional to the heating rate, i.e. a higher heating rate produces less char. However, the process of char formation inside the droplet is not well understood. Therefore, in this work for the sake of simplicity, it is assumed that there is a constant amount of char in each of the particles, i.e. 10 wt.%. Sallevelt [19] used six components to represent pyrolysis oil. However, the goal of the current work is to assess the effect of the solid char on the combustion characteristics. Therefore, to simplify the pyrolysis oil, with the aim of reducing the computational time, only phenol and water (25 wt.%, on liquid weight basis) are taken into account. Particles/droplets loose mass via evaporation and char combustion, which leads to their shrinking. When the total mass of a particle is consumed/converted, this particle disappears from the domain.

The mass, momentum, energy and species conservation equations are solved for the gas phase to calculate the fluid flow, temperature and species distribution in the domain.

$$\frac{\partial \rho}{\partial t} + \nabla(\rho \vec{u}) = \dot{m}'''_{p,g} \tag{9}$$

$$\frac{\partial \rho \vec{u}}{\partial t} + \nabla.(\rho \vec{u}\vec{u}) = -\nabla P + \nabla.(\mu_{eff} \nabla \vec{u}) + \rho \vec{g} + \dot{w}'''_{p,g} \tag{10}$$

$$\frac{\partial}{\partial t}(\rho(h+|\frac{\vec{u}^2}{2}|)) + \nabla.(\rho \vec{u}(h+|\frac{\vec{u}^2}{2}|)) = \nabla^2(\alpha_{eff} h) + \frac{\partial P}{\partial t} + \rho(\vec{u}.\vec{g}) + \dot{q}'''_{p,g} + \dot{q}'''_{reaction} \tag{11}$$

$$\frac{\partial \rho Y_i}{\partial t} + \nabla.(\rho \vec{u} Y_i) = \nabla^2(\mu_{eff} Y_i) + \dot{R}'''_{p,g,i} + \dot{R}'''_{reaction,i} \tag{12}$$

where $\dot{m}'''_{p,g}$ is the mass exchange (sum of all species) between the particles and gas phase, $\dot{w}'''_{p,g}$ is the momentum source due the interactions between two phases, $\dot{q}'''_{p,g}$ is the volumetric heat source which is caused by heat exchange (convection) between the particle and gas phase, $\dot{q}'''_{reaction}$ is the heat source due to the homogeneous reaction in the gas phase, $\dot{R}'''_{p,g,i}$ and $\dot{R}'''_{reaction,i}$ are the species sources $i$ as a result of species exchange between two phases and the gas phase reaction, respectively.

Pyrolysis oil vapor in the gas phase undergoes a homogeneous reaction as follows:

$$C_6H_5OH + 7O_2 \longrightarrow 6CO_2 + 3H_2O \tag{13}$$

The coupling model describes the interaction between particles and environment through heat, mass an momentum transfer. Energy and mass are transferred from the gas to the particles and/or from the particles to the gas as heat source and mass source respectively. The heat and mass source magnitudes are evaluated according to the particle/droplet properties within a specific CFD cell.

## 3. Experimental validation of evaporation model

A literature survey indicates that there are several experimental studies of single droplet pyrolysis oil combustion. However, the required input data necessary for modeling (i.e. boundary and initial condition of the droplet and environment), was not presented in those works. Hence, to validate the numerical model, the predicted results are compared with the experimental data of the evaporation of the droplets containing dissolved solids. Although the combustion process has not been involved in this validation, the main challenge of this work (presence of the solid species in the droplet) is compared against the experimental data.

Evaporation of water droplets containing insoluble solid ($SiO_2$) was studied experimentally by Nesic and Vodnik [25]. They have used individual droplets suspended in a controlled air stream. The droplet weight and the temperature were measured during evaporation. The numerical results have been compared against two experiments with different solid concentrations (30% and 40%) and different operating conditions ($T_{inlet}$ = 101 °C and 178 °C , $u_{inlet}$ = 1.73 $m/s$ and 1.4 $m/s$).

Figure 1 shows good agreement between the measurement and predicted results for both temperature and mass loss. The droplet/particle temperature increases rapidly and remains constant during the evaporation period. When the liquid in the particle is completely evaporated and only solid remains, its temperature increases to the ambient gas temperature. The small deviation between the predicted and measured temperature at the end of evaporation period is caused by crust formation at the outer surface of the droplet/particle. This increases the temperature at the outer solid surface, while there is still liquid at the core of the particle. The crust formation has been neglected in the present model. The results indicate that the numerical model can predict the drying rate, period and temperature with a good level of accuracy.

## 4. Results and Discussion

In this section the results are presented for the combustion of the pyrolysis oil surrogate. In order to study the details of the process on the droplet/particle scale, in the first part, a single droplet/particle combustion process is evaluated. In the second part, the results of the spray combustion of surrogate pyrolysis oil in a typical burner are discussed.

### *4.1. Single droplet combustion*

A single droplet of fuel (phenol 67.5 wt% and water 22.5 wt%) with an initial diameter of 50$\mu m$ containing 10 wt.% solid char at an initial temperature of 320$K$ is subjected to hot air ($T_\infty$ = 1000$K$) with a pressure of 25 $bar$ (char properties are listed in table 1). This is a typical condition that a droplet experiences in a combustor. Figure 2a shows the mass loss of the different species and the temperature of the particle versus time. Since the evaporation period is much shorter compared to the char combustion, the earlier stage of the particle combustion is shown in Fig. 2b to display more details. Because the boiling temperature of water is lower than phenol, evaporation in the particle starts with higher intensity for water. During the water evaporation, the particle temperature is almost constant. At the end of this period the temperature increases gradually and then remains constant at higher temperature where phenol evaporation has high intensity.

During the evaporation period the solid char remains unchanged. After this period, the particle temperature increases rapidly and char combustion starts. As a results of char combustion, the particle temperature goes above the ambient temperature (about 1200 $K$). After some time,

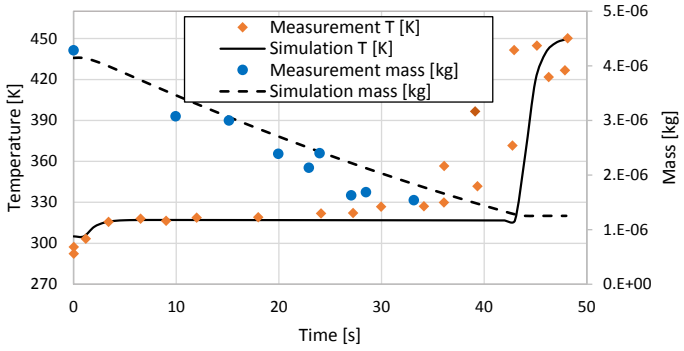


(a)

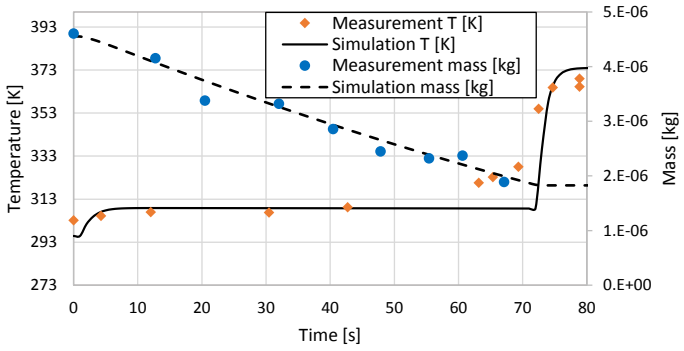


(b)

Figure 1: Experimental validation of the used model. Temperature and mass change of a droplet with solid content during evaporation, a) $T_{inlet}$ = 178 °C, $u_{inlet}$ = 1.4 $m/s$, solid concentration = 30%, diameter= 2.06 mm b) $T_{inlet}$ = 101 °C, $u_{inlet}$ = 1.73 $m/s$, solid concentration = 40%, diameter= 2.06 mm. Experimental data are taken from [25].

it gradually decreases toward the ambient temperature (Fig. 2a). This trend is observed because when the mass of char decreases by burning, it can not produce enough heat to compensate heat loss by convection to the surrounding air flow. Therefore, the cooling effect of the surrounding gas becomes more pronounced and it reduces the particle temperature even though it is still burning.

### *4.2. Spray combustion*

After evaluating a single droplet combustion, the following section describes the behavior of the spray combustion of pyrolysis oil surrogate in a burner. Figure 3 shows schematically the burner with fuel injection at the top-center. The hot air ($T_{in}$ = 1000 $K$) enters to the burner from the top surface and leaves at the bottom surface. The working pressure is 25 bar and the surrounding walls are assumed to ideally have no heat losses. Droplets composition and diameter are similar to the single droplet explained in section 4.1. The burner's dimensions and the diameter of the nozzle are $20 \times 20 \times 100$ $mm$ and 0.19 $mm$, respectively.

Table 1: Char properties

| | |
|---|---|
| Density $\rho$ (kg/ m$^3$) | 2010 |
| Specific heat $c_p$ (J/kg K) | 710 |
| Thermal conductivity $\lambda$ (W/m K) | 0.04 |
| Heat of combustion $H_c$ (kJ/kg) | 32.7 |

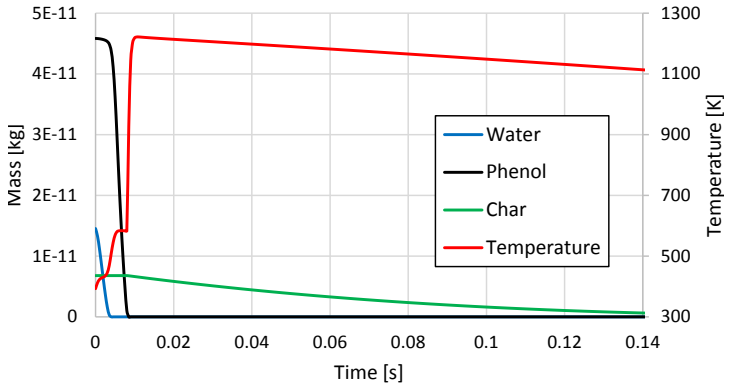


(a)

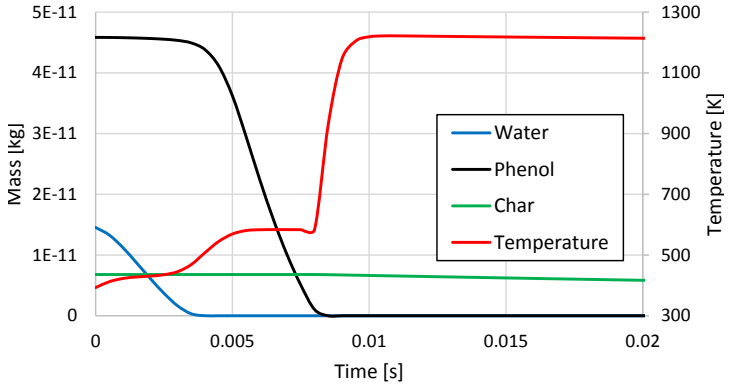


(b)

Figure 2: Temperature and mass loss of phenol, water and char versus time in a single particle by evaporation and combustion ($d = 50\ \mu m$ and $T_\infty = 1000\ K$) a) full process b) zoom on the first 20 ms

The 3D simulation has been repeated for three different grid sizes (40k, 80k and 150k grid). For all three cases, the Courant number has been kept constant and equal to 0.1 during the simulation. The difference between the results from the case with 80k and 150k grid are negligible. Therefore, the 80k grid has been used, further, as the computational effort is less.

Figure 4 depicts the temperature distribution in the gas phase, the phenol content in the particles and the phenol vapor mass fraction in the gas phase at different times. Due to the symmetric flow, in this figure, the temperature distribution is shown in the left half and the vapor

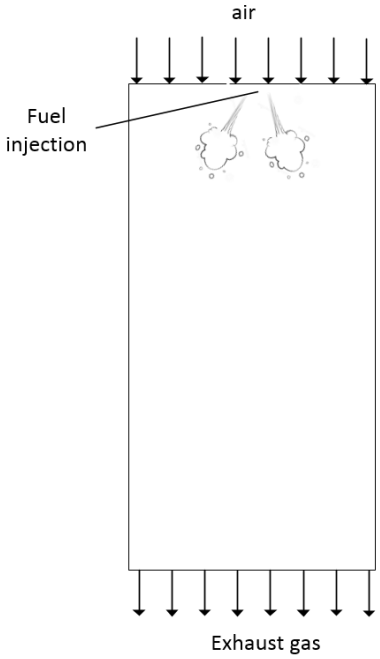


Figure 3: Schematic diagram of the burner.

phenol distribution in the right half.

Phenol in the particles evaporates and is released to the surrounding gas phase. Vapor phenol is distributed in the burner by both diffusion and convective transport and reacts with $O_2$ generating heat. The phenol mass fraction in the particles increases first and then decreases. This is due to the fact that water in the particle evaporates faster than phenol because of its lower boiling point. Although some phenol has been evaporated, the mass fraction of phenol increases in the particles. After the water has evaporated completely, the mass fraction of phenol decreases.

The char remaining in the particle undergoes a heterogeneous oxidation reaction leading to a strong gas and solid temperature increase. At the early stage of the combustion process (Fig. 4a and 4b), phenol vapor is stretched downstream until the end of the particle cloud. Since homogeneous combustion of vapor phenol in the gas phase is faster than heterogeneous combustion of char, most of the oxygen is consumed by the phenol combustion and less oxygen remains for char combustion. Therefore, it can be concluded that most of the heat released at the early stage of combustion comes from combustion of vapor phenol.

At the later stage of combustion (Fig. 4c and 4d), it is observed that about one third of the particle cloud downstream does not have vapor phenol in its surrounding anymore. This means that phenol was combusted completely and the char particles have more chance to meet oxygen and burn. As can be seen in these two figures, the highest gas temperature is at the tail of the particle cloud, where char combustion is more pronounced.

The steady state results of the spray combustion are shown in Fig. 5. The water vapor in the gas phase can come from either evaporation of the particles water content or from the phenol oxidation reaction. The highest value of water vapor mass fraction upstream of the particle cloud

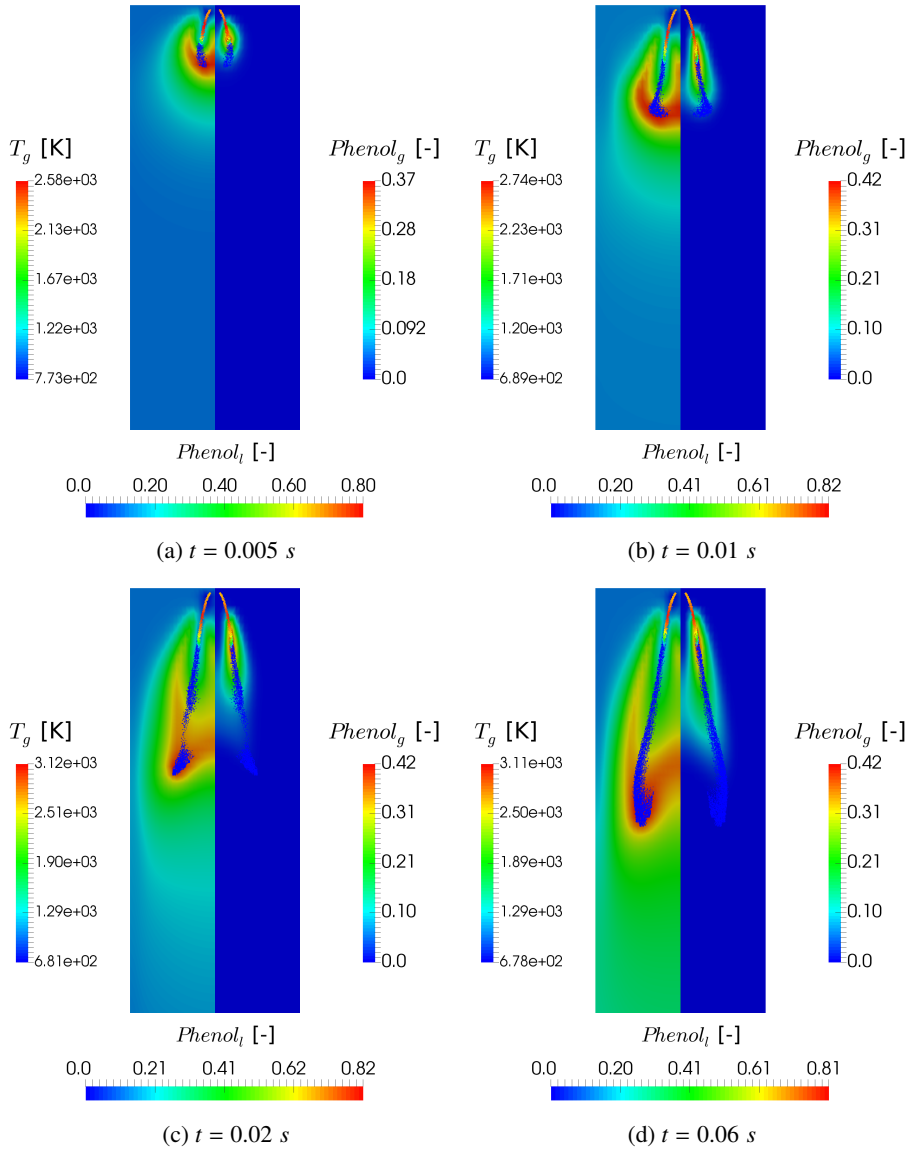


(a) $t$ = 0.005 $s$ (b) $t$ = 0.01 $s$

(c) $t$ = 0.02 $s$ (d) $t$ = 0.06 $s$

Figure 4: Temperature distribution in the gas phase (left side of the figure), liquid phenol mass fraction in the particles and phenol vapor mass fraction in the gas phase (right side of the figure) at different times.

is a result of water evaporation since the phenol combustion is very weak there. $CO_2$ is produced as a result of both phenol and char combustion. The maximum concentration of $CO_2$ in the burner corresponds to the highest temperature in the particles, indicating more dominant $CO_2$ formation during char combustion.

Figure 5a illustrates that the gas temperature decreases close to the injected fuel area, at upstream, due to the heat sink caused by the vaporization of the liquids in the droplet. The figure

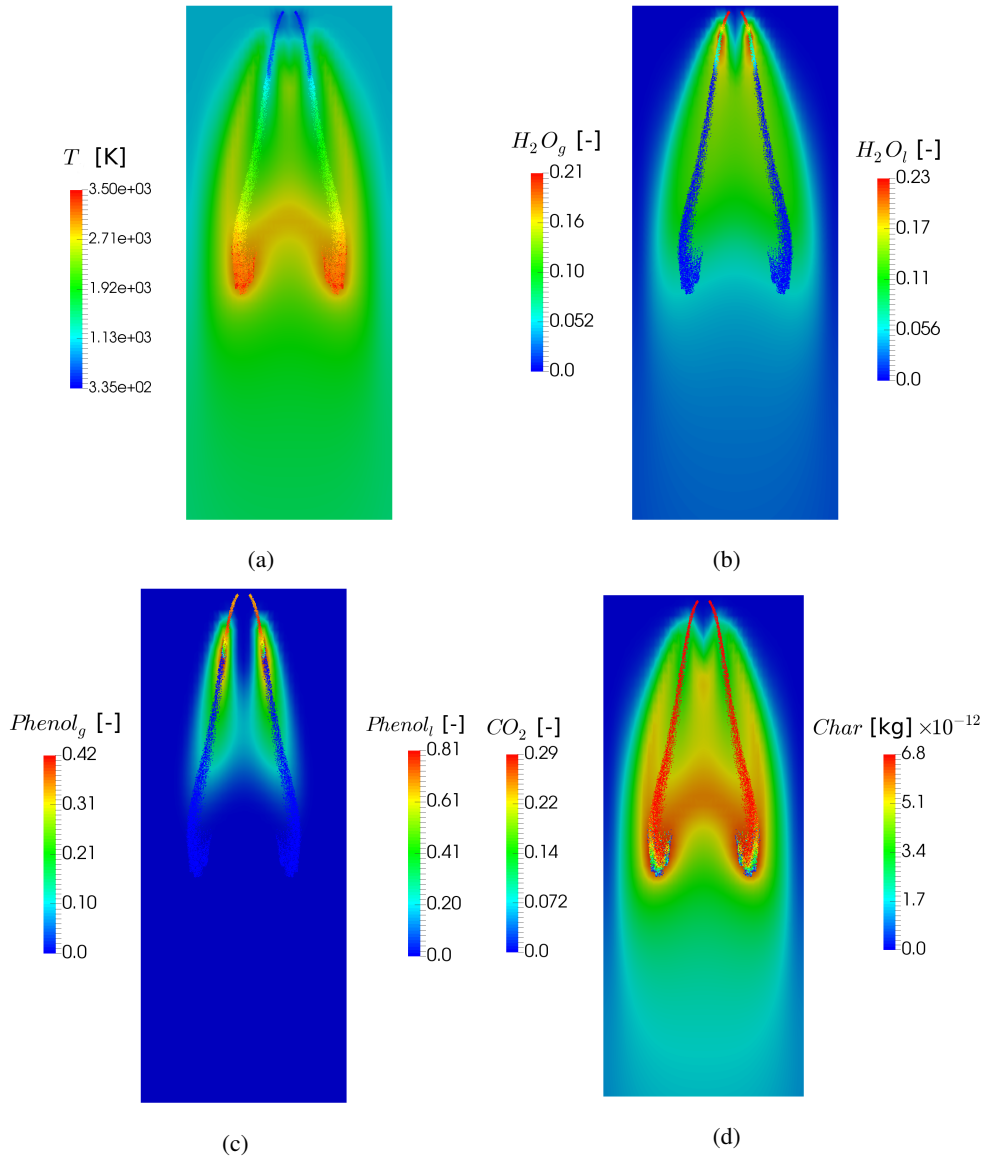


Figure 5: Temperature and species concentrations in the burner at the steady state condition

also shows that the particle temperature during char combustion is considerably higher than the surrounding gas phase temperature. This is caused by the fact that the solid char particles traveling downstream of the burner absorb heat from the hot surrounding gas but there is not enough oxygen to be burned yet. When they reach the zone with higher oxygen concentration, they already have a high temperature (almost close to the gas temperature) and combustion process rise their temperature even more.

Figure 6 depicts the species and the temperature distribution (in the gas phase) along a line at

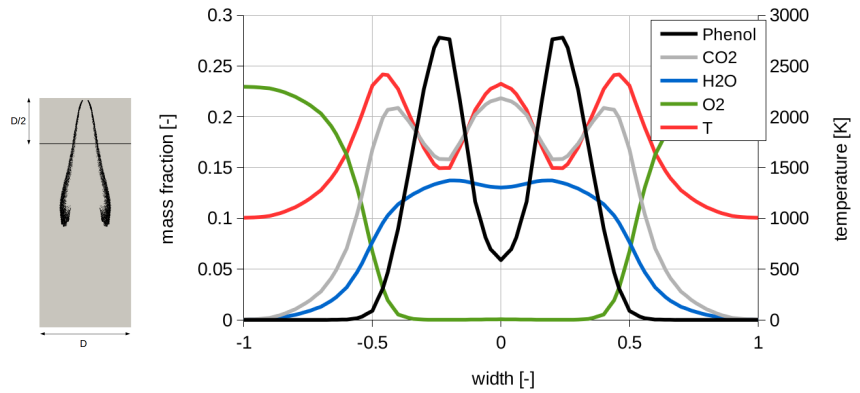


(a)

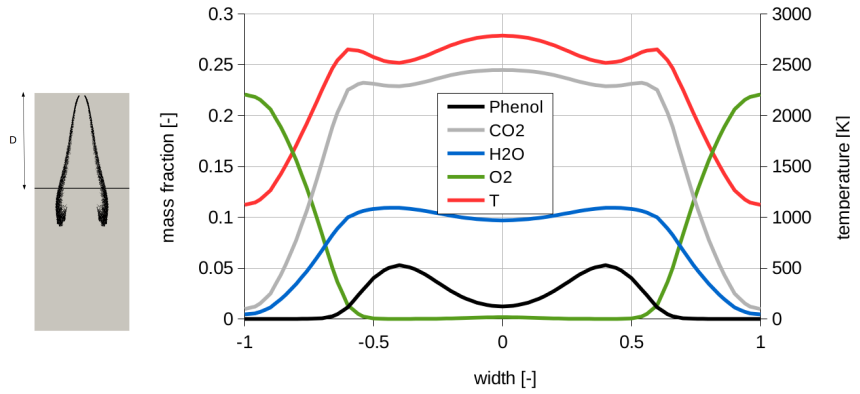


(b)

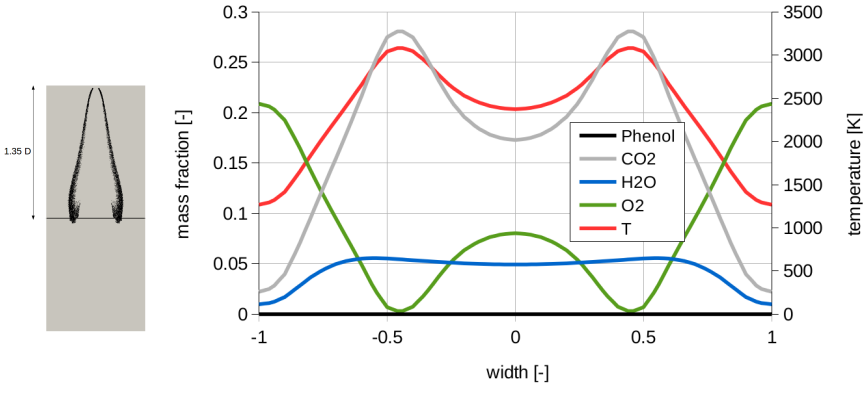


(c)

Figure 6: Temperature and species distribution in the gas phase over horizontal lines at different heights in the burner, as indicated in the left panels

various locations in the burner. Figure 6a shows that there are two peaks of phenol vapor where the line crosses the particle cloud. At those positions, the gas temperature is minimum because of heat loss for the evaporation of liquid in the particles. Phenol vapor is transported downstream to both sides of the particle cloud by convection and diffusion processes, where it mixes with air. Its oxidation leads to a steep reduction in the phenol concentration, and consequently, to an increase of temperature and $CO_2$ content. As can be seen, the phenol mass fraction, unlike the outer side of the particle cloud, does not reach zero between the two particle clouds. This is because there is less oxygen available there leading to a peak with lower temperature compared to two other peaks located in the outer spray region. The water vapor has an almost uniform distribution at the center, because it is produced by both evaporation the droplet and combustion of phenol.

In Fig. 6b, although the phenol vapor concentration is lower than in Fig. 6a, a similar trend for the species and temperature distribution can be observed. However, the gradient is lower and the hot zone is wider. Figure 6c shows that at the line touching the tip of the particle cloud, the phenol mass fraction is equal to zero. There are two temperature peaks where the line crosses the particle clouds, which indicate char combustion. Since the char particles are not very scattered in the gas phase, the combustion and consequently oxygen consumption take place in a narrow band. This leads to the presence of some $O_2$ between the two particle clouds (unlike in Fig. 6a and 6b).

### *4.3. The impact of char formation*

In this section, the already presented results with char are compared with a case where the solid char has been neglected, and therefore only phenol and water are present in the droplet (the 10% char mass is replaced by phenol). The droplets diameter and all the initial and boundary conditions are identical to the previous case. This comparison has been presented in Fig. 7, in which the left half is related to the case with char while the right half shows the results of the case neglecting solid char.

Since there is more phenol (weight basis) in the droplet, in the case without char, it takes longer to evaporate all of it, so its combustion also lasts longer. As can be seen in Fig. 7a, phenol combustion finishes earlier in the case with solid char. The homogeneous reaction of vapor phenol in the gas phase is faster compared to the heterogeneous reaction of the solid char. This changes the hot zone in the case of including char, so that, the combustion region is significantly elongated, Fig. 7c. The results also show that the gas phase reaches a higher temperature when char is present.

Different operating conditions can change the impact of char formation and as consequence its combustion behavior and location. Another drastic impact of char particles in the burner appears if char impinges the burner walls. This might cause fouling and over-heating of the burner's wall leading to serious damage and a failure of the combustion system, however, this was not the scope of this study.

## 5. Conclusions

A numerical model for combustion of multicomponent and multiphase fuels has been developed to study the impact of the existence of solid char on the combustion characteristics. The model is based on an Eulerian-Lagrangian formulation, in which the gas phase is modeled as an Eulerian continuous phase whereas each particle/droplet is tracked with a Lagrangian approach. Each particle consists of two phases (liquid and solid), while it interacts with the surrounding gas

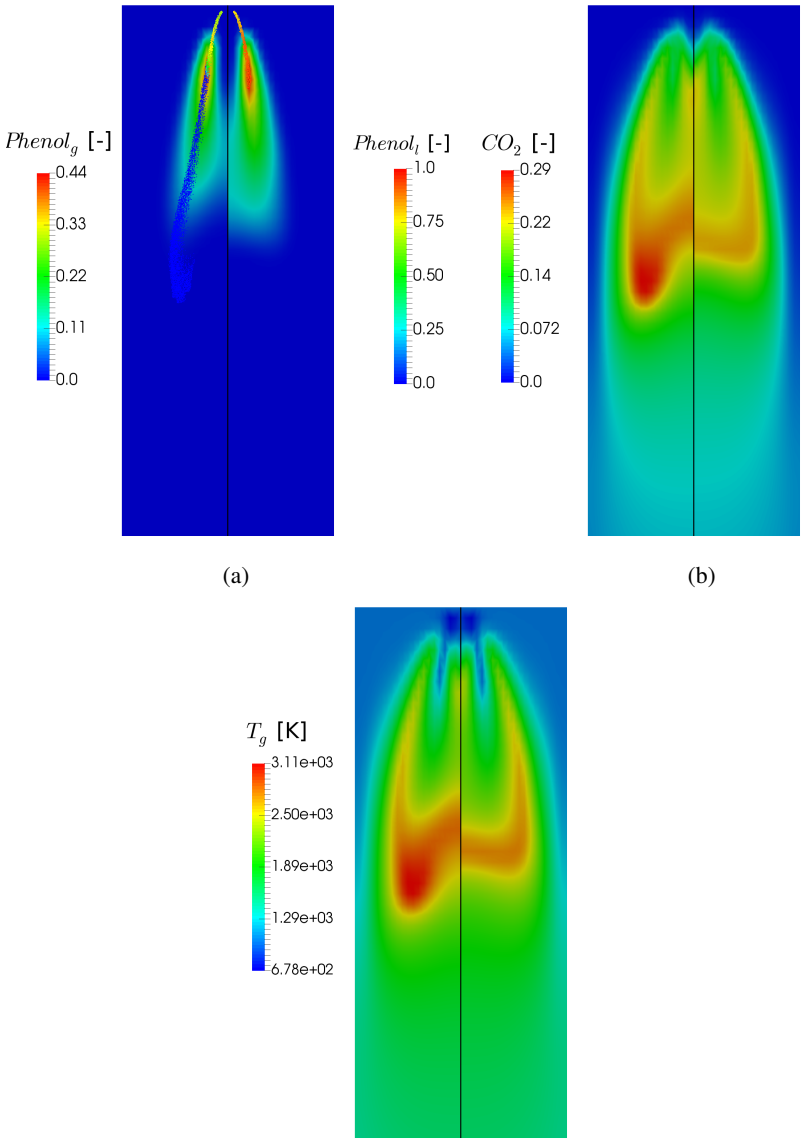


Figure 7: Comparison of temperature and species distribution between cases considering solid char (left half of the figure) and neglecting solid char (right half of the figure)

phase by heat, mass and momentum transfer. The process starts with the evaporation of the liquids in the droplet/particle and it continues by heterogeneous oxidation of the solid residual. The model has been validated against experimental data for the evaporation of a multiphase droplet (water and $SiO_2$) and good agreement has been achieved, however, the combustion would not be validated due to lack of experimental data.

The particle temperature during the char combustion can reach considerably higher values than the gas phase. This causes higher gas temperature due to the downstream char combustion. The homogeneous reaction of vapor phenol in the gas phase is faster compared to the heterogeneous reaction of the solid char. This leads to a change of the hot zone in the burner that should be taken into account in the design process.

## 6. Acknowledgments

The authors would like to thank the Science Based Engineering Institute of the University of Twente for sponsoring this research project (NeMo).

## 7. References

[1] S.-Y. No, Application of bio-oils from lignocellulosic biomass to transportation, heat and power generationa review, Renewable and Sustainable Energy Reviews 40 (2014) 1108 – 1125.
[2] J. D'Alessio, M. Lazzaro, P. Massoli, V. Moccia, Thermo-optical investigation of burning biomass pyrolysis oil droplets, Symposium (International) on Combustion 27 (1998) 1915–1922.
[3] C. Branca, C. D. Blasi, R. Elefante, Devolatilization and heterogeneous combustion of wood fast pyrolysis oils, Industrial and Engineering Chemistry Research 44 (2005) 799–810.
[4] G. van Rossum, B. M. Güell, R. P. B. Ramachandran, K. Seshan, L. Lefferts, W. P. M. V. Swaaij, S. R. A. Kersten, Evaporation of pyrolysis oil: Product distribution and residue char analysis, AIChE Journal 56 (2010) 2200–2210.
[5] B. G. van Rossum, Steam reforming and gasification of pyrolysis oil, Ph.D. thesis, University of Twente (2009).
[6] W. Hallett, N. Clark, A model for the evaporation of biomass pyrolysis oil droplets, Fuel 85 (2006) 532 – 544.
[7] J. D. Brett, A. Ooi, J. Soria, Numerical simulations of an evaporating bio-oil droplet, in: 16th Australasian Fluid Mechanics Conference, 2007.
[8] L. Zhang, S.-C. Kong, Multicomponent vaporization modeling of bio-oil and its mixtures with other fuels, Fuel 95 (2012) 471 – 480.
[9] K. Saha, E. Abu-Ramadan, X. Li, Multicomponent evaporation model for pure and blended biodiesel droplets in high temperature convective environment, Applied Energy 93 (2012) 71 – 79.
[10] S. Sazhin, M. A. Qubeissi, R. Kolodnytska, A. Elwardany, R. Nasiri, M. Heikal, Modelling of biodiesel fuel droplet heating and evaporation, Fuel 115 (2014) 559 – 572.
[11] C. Yin, Modelling of heating and evaporation of n-heptane droplets: Towards a generic model for fuel droplet/particle conversion, Fuel 141 (2015) 64 – 73.
[12] M. J. Wornat, B. G. Porter, N. Y. C. Yang, single droplet combustion of biomass pyrolysis oils, Energy & Fuels 8 (5) (1994) 1131–1142.
[13] R. Calabria, F. Chiariello, P. Massoli, Combustion fundamentals of pyrolysis oil based fuels, Experimental Thermal and Fluid Science 31 (5) (2007) 413 – 420.
[14] S.-S. Hou, F. M. Rizal, T.-H. Lin, T.-Y. Yang, H.-P. Wan, Microexplosion and ignition of droplets of fuel oil/bio-oil (derived from lauan wood) blends, Fuel 113 (2013) 31 – 42.
[15] J. Lehto, A. Oasmaa, Y. Solantausta, M. Kyt, D. Chiaramonti, Review of fuel oil quality and combustion of fast pyrolysis bio-oils from lignocellulosic biomass, Applied Energy 116 (2014) 178 – 190.
[16] M. Beran, L.-U. Axelsson, Development and experimental investigation of a tubular combustor for pyrolysis oil burning, Journal of Engineering for Gas Turbines and Power 137 (2014) 031508–1–7.
[17] M. Wu, S. Yang, Combustion characteristics of multi-component cedar bio-oil/kerosene droplet, Energy 113 (2016) 788 – 795.
[18] J. Hristov, V. Stamatov, Physical and mathematical models of bio-oil combustion, Atomization and Sprays 17 (2007) 731–755.
[19] J. Sallevelt, On the atomization and combustion od liquid biofuels in gas turbines, Ph.D. thesis, university of Twente (2015).

[20] J. Sallevelt, A. Pozarlik, G. Brem, Numerical study of pyrolysis oil combustion in an industrial gas turbine, Energy Conversion and Management 127 (2016) 504 – 514.
[21] T. Forgber, B. Mohan, C. Kloss, S. Radl, Heat transfer rates in sheared beds of inertial particles at high biot numbers, Granular Matter 19 (1) (2017) 14.
[22] W. E. Ranz, W. R. Marshall, Evaporation from drops, Chemical Engineering Progress 48 (1952) 141–146.
[23] D. Spalding, The combustion of liquid fuels, Symposium (International) on Combustion 4 (1) (1953) 847–864.
[24] M. M. Baum, P. J. Street, Predicting the combustion behaviour of coal particles, Combustion Science and Technology 3 (1971) 231–243.
[25] S. Nesic, J. Vodnik, Kinetics of droplet evaporation, Chemical Engineering Science 46 (2) (1991) 527 – 537.